The effects of swirl recovery vanes on single-rotation propeller aerodynamics and aeroacoustics

Sinnige, T; van Kuijk, JJ; Lynch, KP; Ragni, D; Eitelberg, G; Veldhuis, LLM

DOI
10.2514/6.2015-2358

Publication date
2015

Document Version
Accepted author manuscript

Published in
Proceedings of the 21st AIAA/CEAS aeroacoustics conference

The Effects of Swirl Recovery Vanes on Single – Rotation Propeller Aerodynamics and Aeroacoustics

Tomas Sinnige*, Jesse J. A. van Kuijk†, Kyle P. Lynch‡, Daniele Ragni§,

Georg Eitelberg¶, Leo L. M. Veldhuis‖

Delft University of Technology, Delft, 2629 HS, the Netherlands

A preliminary assessment of the aerodynamic and aeroacoustic impact of swirl recovery vanes (SRVs) installed downstream of a single-rotating propeller model was performed at the large low-speed facility of the German-Dutch wind tunnels (DNW-LLF). The SRVs are designed to recover the swirl in the rotor slipstream, thereby increasing the propulsive efficiency without the added complexity of contra-rotating systems. The performance data acquired with a rotating shaft balance showed that the upstream effect of the SRVs on the time-averaged rotor performance was negligible. Particle image velocimetry measurements in the slipstream of the propeller with and without SRVs substantiated the efficacy of the vanes in reducing the swirl in the propeller slipstream. Integrated in the radial direction, installation of the vanes reduced the swirl kinetic energy by 50% at a medium propeller thrust setting. An additional slipstream contraction was observed with vanes installed. The acoustic data measured with out-of-flow microphones showed that installation of the SRVs increased the total sound pressure levels by 2 to 6 dB compared to the isolated propeller.

I. Introduction

The increasing pressure to reduce the fuel burn of civil transport aircraft has renewed interest in propeller propulsion. To maximize the propulsive efficiency of already favorable single-rotating propellers, contra-rotating open rotor (CROR) configurations are an interesting design option. Following an extensive research program led by NASA in the 1980s,[1] it took until the beginning of the 21^{st1} century for research on CRORs to regain momentum. In recent years many studies have been presented in the literature focusing on the aerodynamic and aeroacoustic performance of the isolated CROR, based on both numerical[2,3] and experimental[3,4] methods. In particular, the additional noise emissions resulting from installation of the CROR to the airframe form a popular topic of research, both for semi-installed[5–7] and fully-installed configurations.[8–10]

When designing a propeller for the transonic cruise Mach number of today's passenger transport aircraft, aerodynamic and aeroacoustic considerations impose limits on the blade tip Mach number. Taking into account the high inflow velocity, this requires the rotational speed to be reduced. Consequently, the propeller disk loading will need to be relatively high compared to the more lightly-loaded propellers designed for lower cruise Mach numbers. As a result, the swirl losses in the propeller slipstream are increased, reducing the propulsive efficiency. By employing a second rotating blade row, contra-rotating propellers can recover this swirl energy, thereby increasing the propulsive efficiency in cruise by up to 8%.[11] As shown by the same study, this however comes at the cost of increased weight and complexity.

Considering a design solution with a stationary second rotor, effectively a stator is obtained for which an efficiency gain can still be achieved, however without the added complexity associated with contra-rotating systems. In the early nineties such a configuration was studied by NASA and associated research partners,

*Ph.D. Student, Flight Performance and Propulsion Section, Faculty of Aerospace Engineering, AIAA member.
†M.Sc. Student, Flight Performance and Propulsion Section, Faculty of Aerospace Engineering.
‡Ph.D. Student, Aerodynamics Section, Faculty of Aerospace Engineering, AIAA member.
§Assistant Professor, Wind Energy Section, Faculty of Aerospace Engineering, AIAA member.
¶Full Professor, Flight Performance and Propulsion Section, Faculty of Aerospace Engineering, AIAA member.
‖Full Professor, Head of Flight Performance and Propulsion Section, Faculty of Aerospace Engineering, AIAA Member.

who introduced the term Swirl Recovery Vanes (SRVs) for the fixed downstream blade row.[12–15] Wind tunnel tests confirmed the potential efficiency increase resulting from application of the SRVs, with measured efficiency gains of around two percent.[12] At the same time, numerical analyses based on solutions of the Euler equations predicted an efficiency increase of approximately five percent for the same configuration and operating conditions.[13,14] No additional noise was measured compared to the propeller configuration without the SRVs, while depending on the SRV design and the operating conditions even a reduction in noise was observed due to unloading of the front blade row.[15] Apart from the work performed by NASA and partners in the 1990s, more recently a CFD analysis using a RANS solver showed increased thrust levels due to application of the SRVs.[16] However, in the same study it was shown that the total system efficiency was reduced, stressing the importance of proper SRV design and integration.

Considering the limited number of studies devoted to SRVs published as of now, the effect of the SRVs on the aerodynamic and aeroacoustic performance of propeller propulsion systems is still largely unclear. The experimental study discussed in this paper was part of the initial phase of ongoing research on swirl recovery systems for propeller applications at Delft University of Technology. It was aimed at comparing the aerodynamic and aeroacoustic performance of a modern high-speed propeller with and without downstream swirl recovery vanes. The measurements were executed as a secondary part of the test program of the APIAN-INF experiment, the main objective of which was the quantification of the effects of pylon blowing on pusher propeller installation as discussed in Ref. 17. The test was performed in the EU-funded ESWIRP project, and involved contributions from Airbus, Delft University of Technology, DLR, DNW, INCAS, TsAGI, TU Braunschweig, and the University of Cambridge.

II. Experimental Setup and Methodology

A. Wind Tunnel Facility and Models

The measurements were performed at the large low-speed facility (LLF) of the German-Dutch wind tunnels (DNW). The dimensions of the test hall are around 50 m x 30 m x 20m, while an open jet configuration was selected with 8 m x 6 m outlet. The tunnel flow's turbulence level is below 0.02%, while the total pressure deviations at the position of the models are smaller than 0.1%. The test hall is equipped with acoustic lining to achieve semi-anechoic conditions. The low background noise levels of the tunnel were further improved by recent upgrades of the turning vane geometry and the heat exchanger – flow straightener assembly.[18]

A modern tractor propeller model was used together with detachable SRVs to perform tests for the cases with and without the SRVs installed. A photograph of the test setup is shown in Fig. 1.

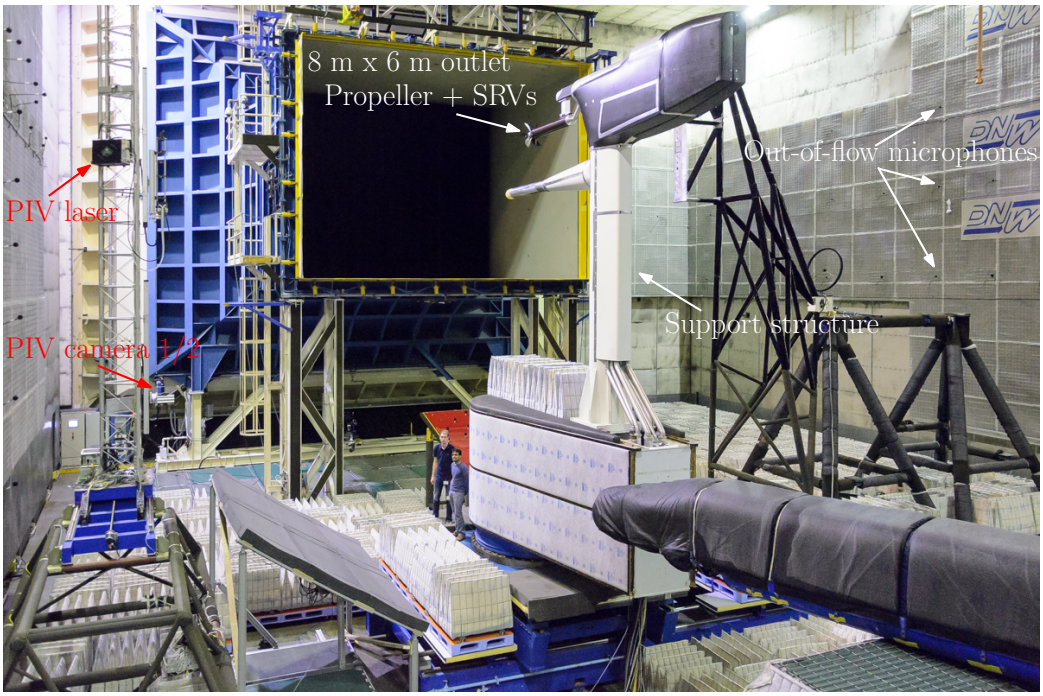

Figure 1. Photograph of the experimental setup, showing the propeller and swirl recovery vanes installed on the fixed support structure.

The six-bladed propeller model with a diameter of 0.508 m was originally developed for the European APIAN (Advanced Propulsion Integration Aerodynamics and Noise)[19–22] project. The blade angle was set to a fixed value of 40.4 degrees at 75% of the radius. A photograph of the propeller model is presented in Fig. 2.

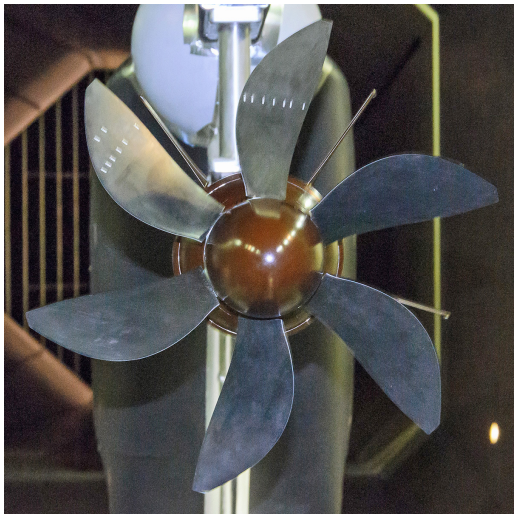

Figure 2. Front view of the APIAN propeller model with swirl recovery vanes installed.

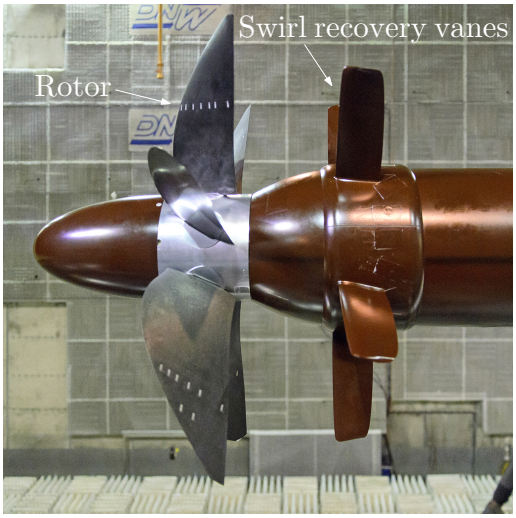

Figure 3. Side view of the APIAN propeller model with swirl recovery vanes installed.

The geometry of the swirl recovery vanes was defined using the first generation of an in-house developed low-order design method based on the propeller analysis and design program XROTOR[23]. Initially, the velocity components in the slipstream of the simulated APIAN propeller were computed under the assumption that they were unaffected by the downstream SRVs. With the inflow velocity field on the SRVs known, XROTOR's minimum induced loss design routine was applied to generate the SRV design. The upstream influence of the SRVs on the rotor was then used to recompute the propeller slipstream, after which the SRV design was updated. A number of such design iterations were performed until the results converged. The axial velocities in the propeller slipstream predicted using XROTOR were within 5% of the values measured previously using particle image velocimetry (see Ref. 21). For the tangential components the difference was larger, with deviations ranging from 5% at the inboard sections to 30% near the tip of the propeller. A design rotor advance ratio of $J = 1.75$ was selected, based on the requirement for the system to offer good performance in cruise conditions. To reduce interaction noise a total of five vanes was chosen, while the diameter of the SRVs was set to 90% of that of the front rotor to prevent additional noise due to blade-vortex interactions. Furthermore, a NACA 0009 cross-section was selected for the entire vane as it offered the best performance in terms of the predicted system efficiency gain of the airfoils considered in the optimization process. The spacing between the front rotor and the SRVs was equal to approximately 30% of the propeller diameter. A photograph of the SRVs installed downstream of the APIAN propeller is shown in Fig. 3.

B. Experimental Techniques

The impact of the SRVs on the propeller propulsive performance, slipstream flow fields, and noise emissions was assessed using several measurement techniques. The propeller model included a three-spoke, six-component rotating shaft balance (RSB) which measured the propulsive performance during operation. The thrust and torque were acquired directly, while the remaining forces and moments were reconstructed from the two in-plane components recorded with the RSB.

The aerodynamic effects of installation of the SRVs on the propeller slipstream were quantified using stereoscopic PIV. The measurements were performed in a number of longitudinally adjacent planes at the vertical position of the propeller axis. Post-processing was performed for these planes separately, after which the results were combined to obtain the final flow field data. Figure 4 illustrates the size and position of the measurement domain relative to the model. Phase-locking was applied at eleven different angular blade positions, separated by six degrees. Fifty images were taken per phase angle, which were averaged to obtain the mean flow fields. Table 1 provides an overview of the most important characteristics of the PIV setup.

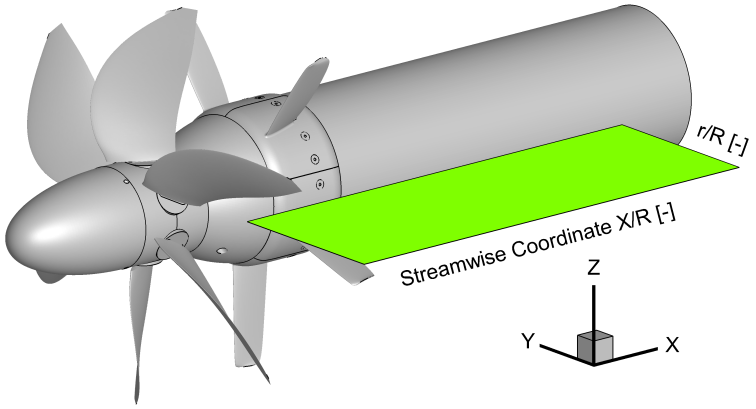

Figure 4. Schematic indicating the size and position of the combined measurement plane used for the PIV evaluations of the propeller slipstream.

Table 1. PIV setup and data acquisition characteristics.

Parameter	Value
Laser	Quantel Evergreen Nd:YAG 200 mJ
Cameras	2x PCO SensiCam
Image sensor size	1,280 px x 1,024 px
Pixel size	6.7 μm x 6.7 μm
Objective	Zeiss 200mm f/2.0 + 2x teleconverter
Effective focal length	400 mm
Effective aperture	f/4.0

Parameter	Value
Magnification	0.040
Digital resolution	6.0 px/mm
Pulse separation	$15 - 20$ μs
Freestream shift	$5 - 7$ px
Phase angle separation	6 deg
Samples per phase angle	30

The change in aeroacoustic performance resulting from the installation of the SRVs was measured using 48 out-of-flow microphones, installed on the wall of the test hall. The microphones covered a range of axial and circumferential directivity angles, which were defined following the schematic given in Fig. 5. Half of the microphones were mounted at the height of the propeller axis, corresponding to a circumferential directivity angle of approximately 0°. The remaining 24 microphones were divided equally between vertical positions above and below the propeller, corresponding to circumferential directivity angles of $-10°$ and $+10°$. At each circumferential directivity angle, an axial directivity range was covered of approximately $35° \leq \theta \leq 145°$, not taking into account shear layer refraction effects.

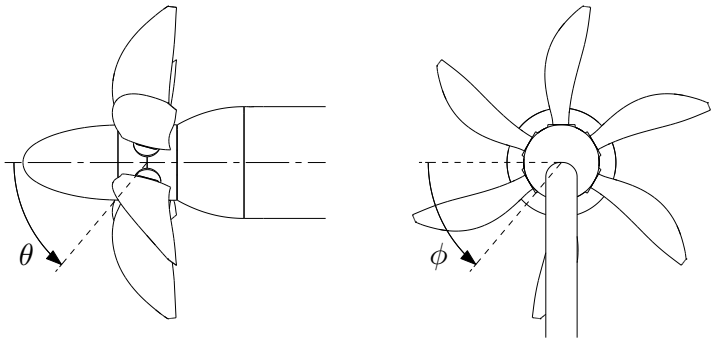

Figure 5. Definition of axial and circumferential directivity angles θ and ϕ.

C. Analyzed Test Cases

The measurements were performed for various different operating conditions. An overview of the analyzed test cases is given in Table 2. The three propeller advance ratios considered for the slipstream flow field and acoustic measurements ($J = 1.05, 1.40, 1.75$) were selected to simulate a "high", "medium", and "low" thrust setting, respectively. Complete propeller performance maps were obtained by also considering additional advance ratios during dedicated RSB measurement runs. All measurements were performed in symmetric inflow conditions ($\alpha = \beta = 0°$).

Table 2. Overview of the analyzed test cases.

Parameter	Symbol	Value
Freestream velocity	U_∞	60 m/s
Advance ratio	J	1.05, 1.40, 1.75
Angle of attack	α	0°
Angle of sideslip	β	0°

III. Results

A. Propeller Propulsive Performance

The propulsive performance of the propeller model was monitored using the RSB during all measurements. The SRVs were not instrumented, hence no information was available of their contribution to the total system thrust and efficiency. The forces and moments generated by the propeller itself were expressed by a thrust coefficient C_T, torque coefficient C_Q, and propeller efficiency η, defined as:

$$C_T = \frac{T}{\rho_\infty n^2 D^4} \quad (1) \qquad C_Q = \frac{Q}{\rho_\infty n^2 D^5} \quad (2) \qquad \eta = \frac{J}{2\pi}\frac{C_T}{C_Q} \quad (3)$$

with D the propeller diameter, J the advance ratio ($J = \frac{U_\infty}{nD}$), n the rotational speed of the propeller in revolutions per second, Q the propeller torque, T the propeller thrust, and ρ_∞ the freestream density.

The propeller propulsive performance diagrams acquired with and without the SRVs installed are depicted in Fig. 6. Estimations of the variation of repeated measurements were made by considering the multiple data points obtained at the three advance ratios considered for the largest part of the test program (see Table 2), and are indicated by the error bars. At an advance ratio of $J = 1.05$ a variation of 1% of the measured thrust coefficient was found, whereas at the lower thrust setting corresponding to $J = 1.75$ the variation of the acquired thrust coefficient equaled 5%.

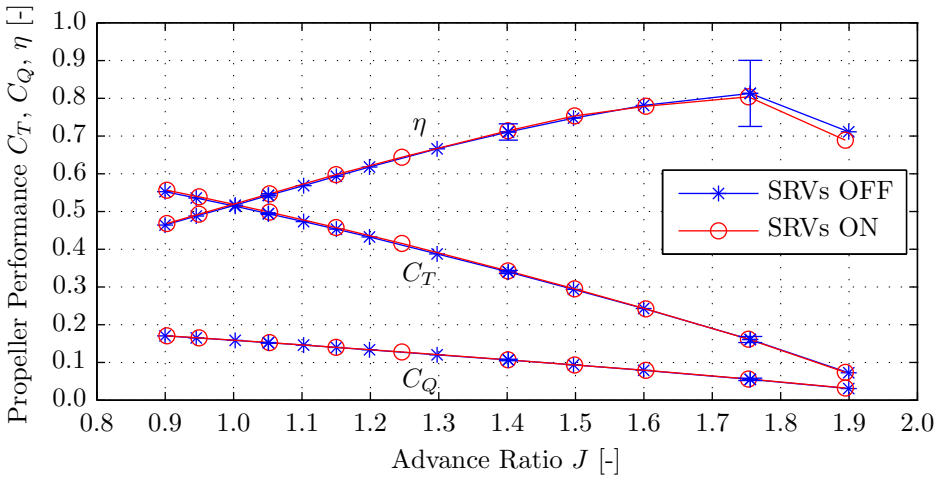

Figure 6. Effects of installation of the swirl recovery vanes on the propeller performance.

Figure 6 shows that the effect of installation of the SRVs on the performance of the propeller is negligible. For all advance ratios the change in performance remains within the statistical uncertainty of the measurements, with a difference of at most 1% compared to the performance of the isolated propeller. This implies that the upstream effects of the SRVs on the rotor are negligible. This is as expected considering the relatively small ratio of the loads generated by the vanes relative to the rotor. The fact that the efficiency of the propeller itself did not change appreciably as a result of the installation of the SRVs indicates that a net gain in system propulsive efficiency was achieved if the vanes were generating positive thrust.

B. Slipstream Flow Fields

To quantify the aerodynamic effects of the SRVs on the propeller slipstream, the flow downstream of the propeller with and without swirl recovery vanes was evaluated using PIV. Figure 7 presents the slipstream flow fields behind the isolated propeller, at all eleven phase angles considered. Vorticity isosurfaces are plotted together with contours of the difference between the local and freestream axial velocity components. Note that all measurements were performed in the single measurement plane indicated in Fig. 4. However, because of the rotational symmetry of the isolated propeller configuration the results acquired in the single measurement plane could be rotated with the relative blade phase angle to obtain the visualization presented in Fig. 7.

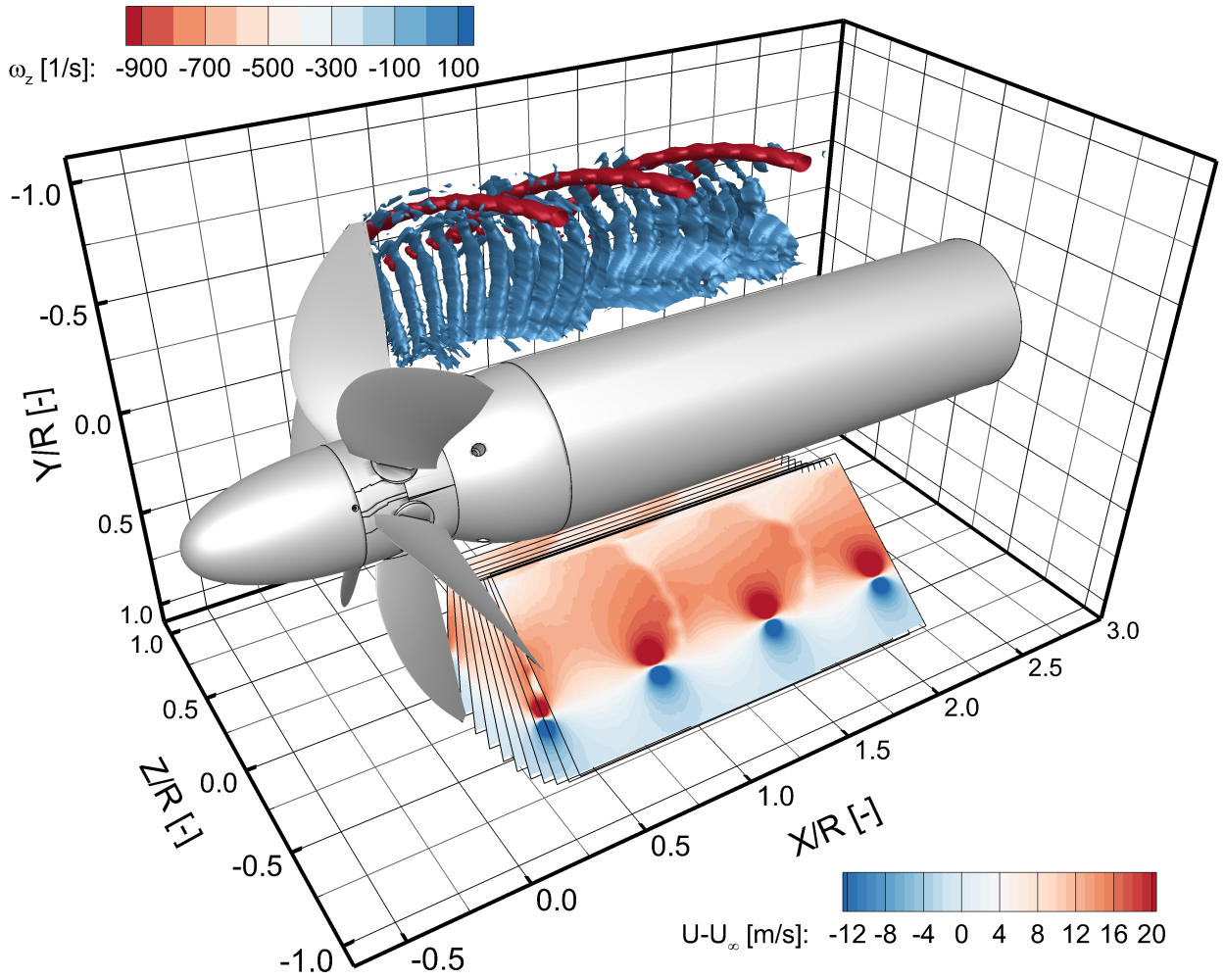

Figure 7. Contours of streamwise velocity component with freestream value subtracted (bottom left) and vorticity isosurfaces (top right) measured for the isolated propeller; $J = 1.40$.

The vorticity isosurfaces shown in Fig. 7 display the helicoidal system of blade tip vortices and wakes, resulting from the swirl in the slipstream of the isolated propeller. The velocity fields confirm the expected axial velocity increase in the propeller slipstream, except in the clearly captured blade wake regions.

The purpose of the installation of the SRVs is to recover the swirl in the propeller slipstream, thereby increasing the efficiency of the propulsion system. To quantify the amount of swirl present in the propeller slipstream, a swirl kinetic energy ratio ϵ_k is defined as:

$$\epsilon_k = \frac{E_k^{swirl}}{E_k^{\infty}} = \frac{V^2 + W^2}{U_{\infty}^2} \tag{4}$$

with U, V, and W the streamwise, lateral, and vertical velocity components, respectively.

Figure 8 presents contours of the swirl kinetic energy ratio defined by Eq. (4) for the configurations with and without the SRVs installed. The phase-averaged results are considered, for the propeller operating at a medium thrust setting ($J = 1.40$). Radial distributions of the swirl kinetic energy ratio were extracted at streamwise positions upstream and downstream of the vanes, and are plotted in Fig. 9.

Figures 8 and 9 confirm the decrease in swirl kinetic energy in the propeller slipstream obtained by installation of the SRVs. Downstream of the vanes a reduction of up to 95% is achieved in the most inboard part of the slipstream. With increasing radial coordinate the amount of swirl recovery decreases linearly to zero around the blade tip. Integrated over the entire radial domain considered, the presence of the SRVs reduces the swirl kinetic energy by 50%.

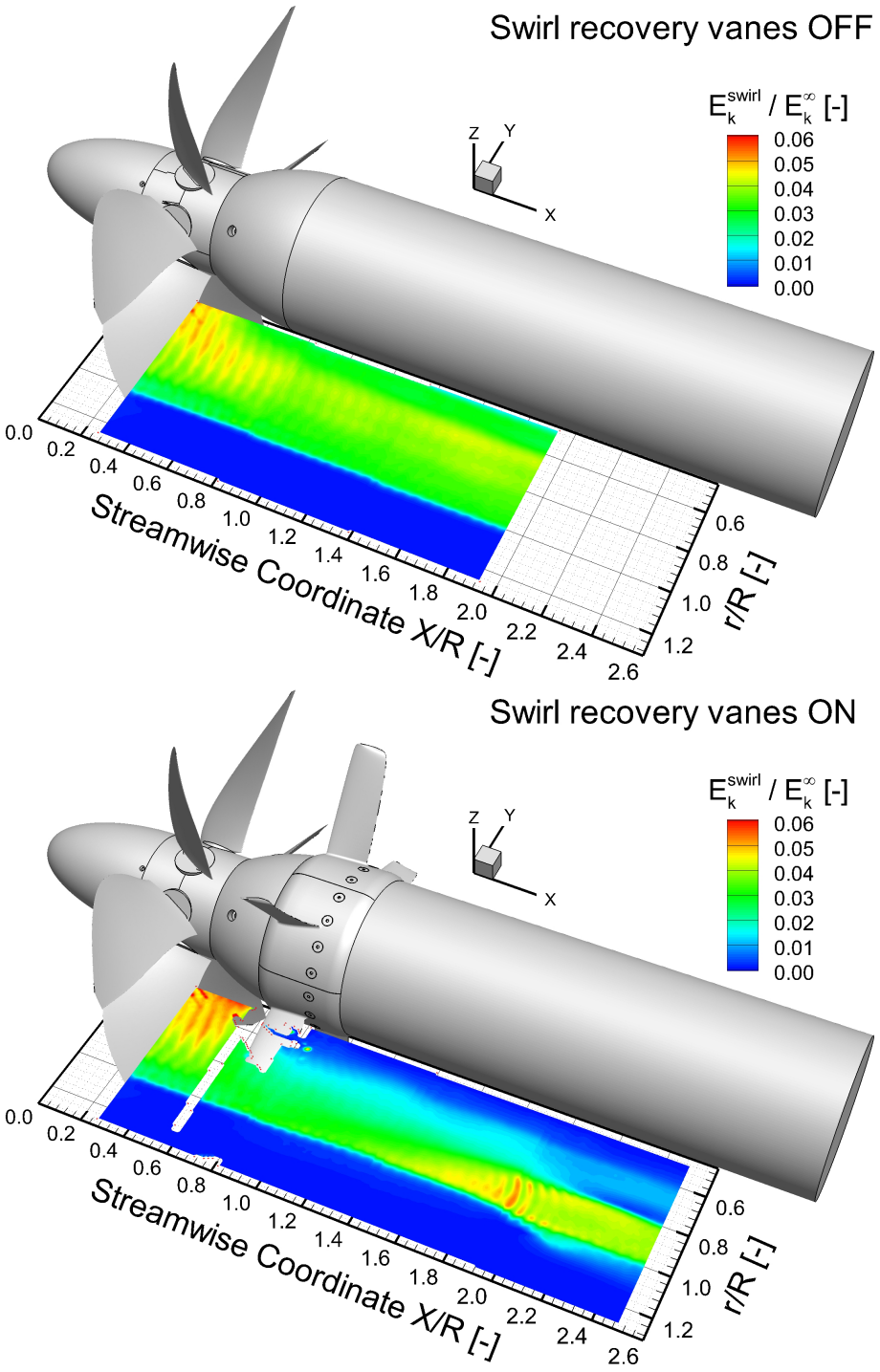

Figure 8. Phase-averaged swirl kinetic energy ratio with and without swirl recovery vanes installed; $J = 1.40$.

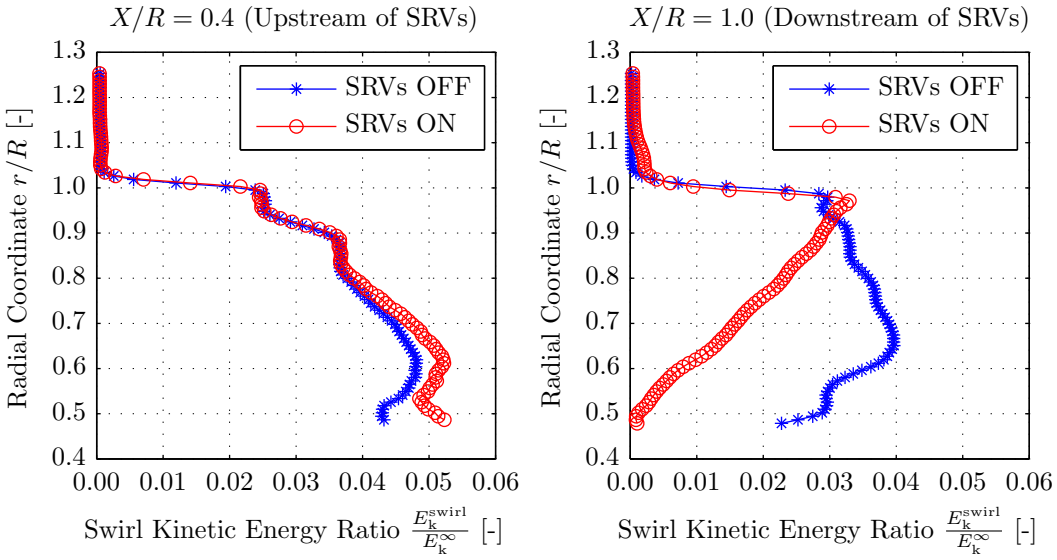

Figure 9. Swirl kinetic energy ratio profiles with and without swirl recovery vanes, installed at streamwise positions upstream (left) and downstream (right) of the vanes; $J = 1.40$.

Upstream of the SRVs the swirl is increased due to the presence of the SRVs, which is the result of the upwash generated by the lifting vanes. From a streamwise coordinate of around $X/R = 1.8$ onwards one of the SRVs' tip vortices crosses the measurement plane. The resulting interaction with the tip vortex of the main rotor locally increases the swirl. Note that the installation of the SRVs removes the axisymmetry of the flow field, hence the single PIV plane does no longer provide an integral view of the entire slipstream as for the isolated propeller.

The goal of installation of the SRVs is to convert the momentum in the swirl directions into an additional axial momentum component, thereby increasing the thrust of the propulsion system. Since the shaft power will remain unchanged, as confirmed by the results presented in Subsection A, in this way the overall propulsive efficiency is increased. The change in axial momentum due to the axial velocity component was studied by analyzing the axial velocity profiles and slipstream radii with and without SRVs installed. The axial velocity profiles were extracted at the same streamwise locations as used in Fig. 9, and are presented in Fig. 10. As mentioned previously, with SRVs present the single PIV plane cannot provide an integral picture of the slipstream flow field. Therefore, the results presented in Fig. 10 cannot be used to quantify the gain in thrust obtained by installation of the SRVs.

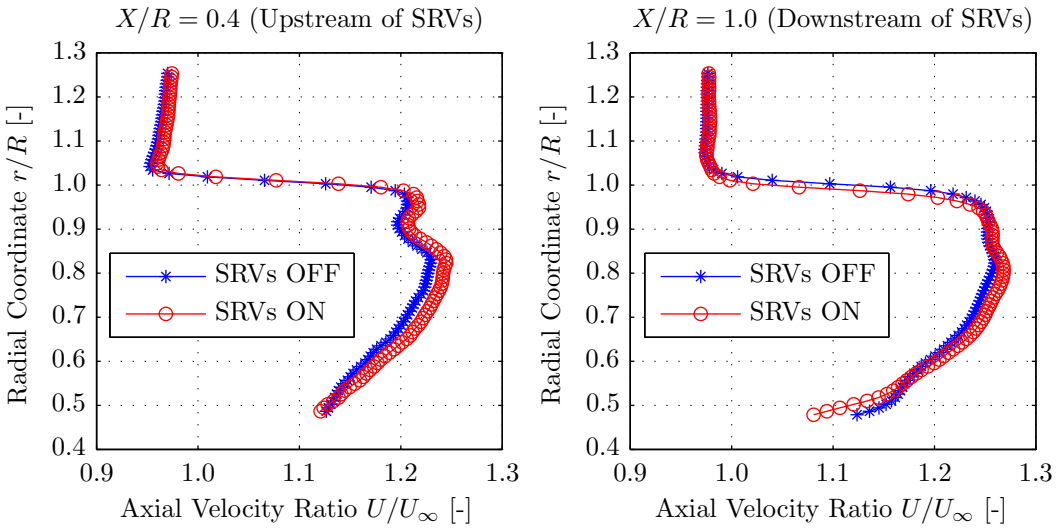

Figure 10. Axial velocity profiles with and without swirl recovery vanes installed at streamwise positions upstream (left) and downstream (right) of the vanes; $J = 1.40$.

Figure 10 shows that with SRVs installed, downstream of the vanes an increase in axial velocity of at maximum 1% is obtained for $0.5 < r/R < 0.9$. At the most inboard stations a reduction in axial velocity is seen for the configuration with SRVs present. This is due to the reduction in swirl obtained by installation of the vanes, which resulted in a longitudinal stretching of the propeller blade wake regions in the measurement plane. Hence, the average velocity over all phase angles was lower at the inboard radial stations with the SRVs installed.

To preserve the mass flow in the propeller slipstream, any increase in axial velocity should lead to a contraction of the slipstream. Therefore, to further quantify the changes in axial velocity in the propeller slipstream due to installation of the SRVs, the positions of the slipstream edge were extracted from the PIV data. In this process the position of the slipstream edge was defined at the radial coordinate of the maximum absolute value of the vorticity at each streamwise position X/R. Figure 11 presents the corresponding results for all propeller operating points considered. The increase in the hub radius directly downstream of the propeller (see Figs. 2 and 3) results in an outward movement of the propeller slipstream. Therefore the radial coordinates of the slipstream edge given in Fig. 11 cannot be used to compute the overall slipstream contraction relative to the propeller diameter at $X/R = 0$.

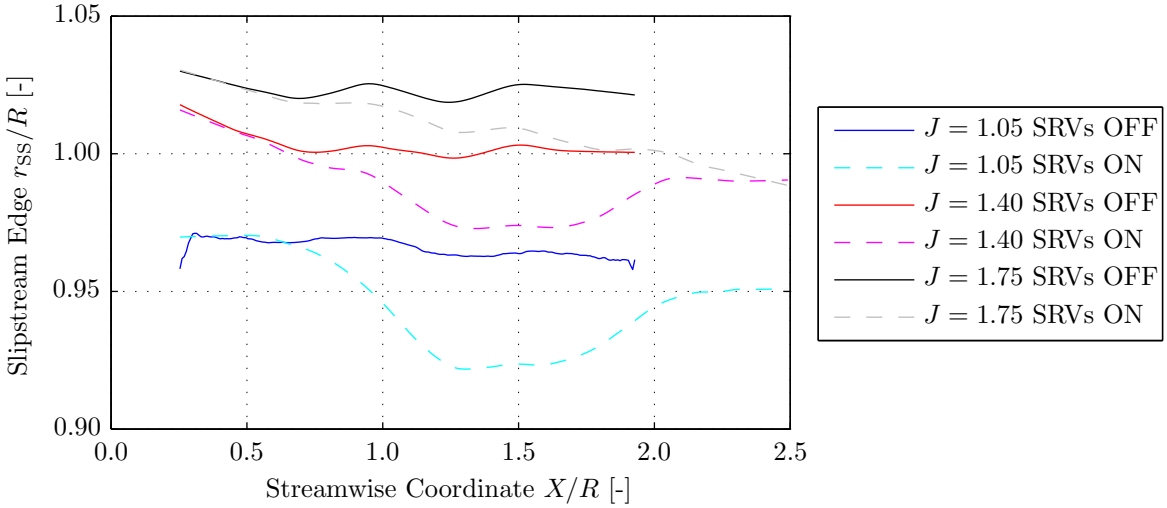

Figure 11. Slipstream edge positions for the cases with and without swirl recovery vanes installed.

The radial coordinates of the slipstream edges shown in Fig. 11 decrease with increasing propeller thrust setting, as expected. For the isolated configuration a minor contraction is observed at all advance ratios, but the rotor's tip vortices remain clear of the vanes. Compared to the results for the isolated propeller, installation of the SRVs clearly moves the slipstream edge in the inboard direction, indicating an acceleration and thus a potential increase in thrust. For the case with SRVs on, at $J = 1.05$ and $J = 1.40$ a tip vortex from one of the SRVs crosses the measurement plane at $X/R = 1.3$ and $X/R = 1.8$, respectively. The corresponding increases in the radial coordinate of the slipstream edge are due to the resulting interaction with the rotor blade tip vortices. This confirms once more that the results obtained in the single measurement plane cannot be used to draw conclusions about the overall thrust gain obtained by installation of the vanes.

C. Propeller Noise Emissions

Similarly as for CRORs, compared to a single-rotating propeller the installation of the SRVs introduces additional noise generating mechanisms due to interactions between the rotor and the downstream SRVs. Since the SRVs are not rotating, the additional noise will consist of tonal components with frequencies equal to multiples of the rotor's blade passage frequency (BPF). To assess the noise penalty due to installation of the SRVs, Fig. 12 presents the sound spectra for the cases with and without the SRVs as measured by the out-of-flow microphone in the propeller plane. These data are presented as measured, no corrections have been performed for shear layer refraction effects and no normalization has been applied to scale the sound pressure levels to a desired source-observer distance. The sound pressure levels are plotted versus multiples of the propeller BPF on the horizontal axis. For the operating conditions considered in Fig. 12 the BPF equals 509 Hz.

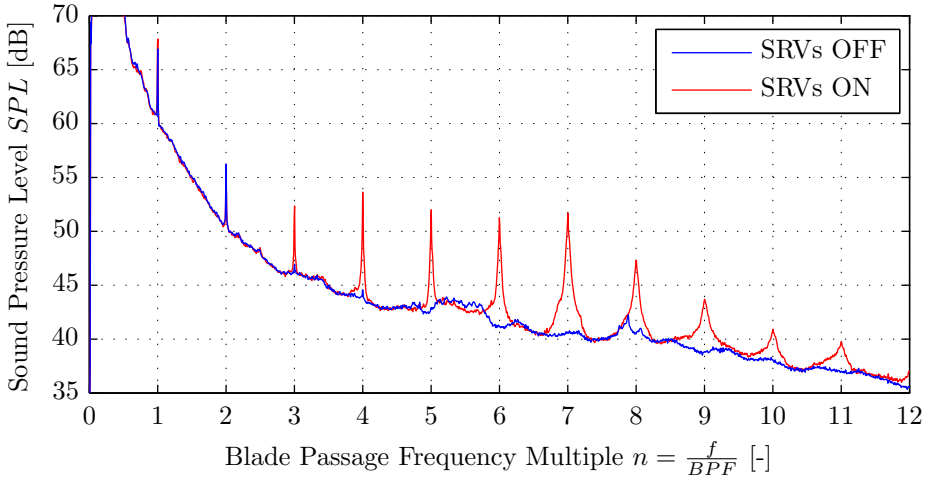

Figure 12. Out-of-flow microphone sound spectra with (SRVs on) and without (SRVs off) swirl recovery vanes; $\theta = 90°$, $\phi = 0°$, $J = 1.40$.

Figure 12 indicates that both with and without SRVs the sound spectrum is dominated by the fundamental tone (1·BPF). The installation of the SRVs increases the sound pressure level of this tone by almost 2 dB. Although at levels much lower than that of the fundamental tone, with noise penalties of up to 12 dB the increase in noise levels of the higher harmonics is much more pronounced. This matches with an analysis of the modal efficiencies following the analytical model for propeller noise emissions presented in Ref. 24. For higher harmonics of the BPF, a larger number of (higher order) wake harmonics contribute to efficiently radiating modes. For the isolated propeller on the other hand the steady loading and thickness sources are radiated efficiently mainly at the fundamental frequency, after which the SPL rapidly decreases for the higher harmonics.

The sound spectra presented in Fig. 12 display data for a single microphone only. To identify the trends in noise penalty due to installation of the SRVs versus the axial and circumferential directivity angles, Fig. 13 depicts the change in total tonal sound pressure level due to the presence of the SRVs for all out-of-flow microphones. The sound pressure levels measured for the isolated propeller are taken as baseline. The total tonal sound pressure level is defined as the sum of the SPL of all measured propeller tones.

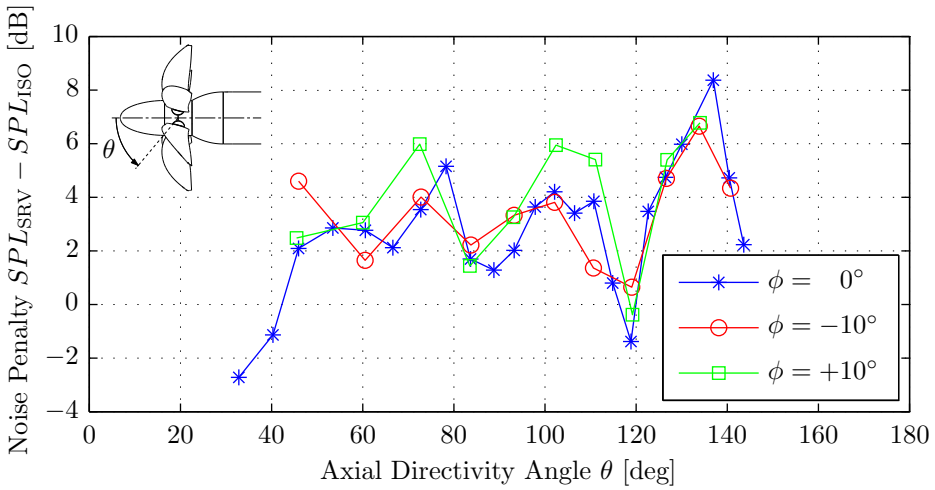

Figure 13. Noise penalty due to installation of the SRVs for all out-of-flow microphones; $J = 1.40$.

Figure 13 shows comparable trends at the three different circumferential directivity angles, with noise increases due to installation of the SRVs of about 2 to 6 dB for most of the axial directivity range. The increase in the sound pressure level due to the installation of the SRVs contradicts with the findings presented in Ref. 15, in which no noise penalty is reported. However, compared to the experiment discussed in the present manuscript, the measurements treated in Ref. 15 were performed at much higher tip Mach numbers, with a larger rotor blade count, and a larger rotor - stator spacing. These are all considered as noise reducing parameters for rotor-stator interaction noise.[25,26]

The additional noise with the SRVs installed results from the addition of two noise generating mechanisms compared to the isolated propeller without the vanes. The downstream interaction of the vanes with the wakes of the propeller blades leads to unsteady pressure perturbations on the swirl recovery vanes, hence additional noise. At the same time the upstream potential effect of the vanes on the propeller blades leads to unsteady rotor loading, with associated noise emissions. However, due to the small fraction of the total load generated by the SRVs compared to the rotor and the relatively large spacing between the propeller and the vanes, this upstream effect is expected to be small. This was also shown by the RSB measurements of the propeller propulsive performance discussed in Subsection A. The reduced noise emissions in the most upstream part of the domain shown in Fig. 13 could be the result of interference between the various noise sources. Note that the aeroacoustic performance was not considered in the design optimization of the vanes.

IV. Conclusions & Outlook

The aerodynamic and aeroacoustic effects of the installation of swirl recovery vanes downstream of a single-rotating propeller model were studied in a large-scale wind tunnel. Based on the results discussed in this manuscript the following conclusions were drawn:

- The installation of the SRVs did not result in measurable changes in the integral propeller performance parameters over the complete advance ratio range considered. Hence, it is concluded that the upstream effect of the swirl recovery vanes on the time-averaged propeller performance is negligible.
- From a comparison of the propeller slipstream flow fields with and without SRVs it is concluded that installation of the vanes indeed resulted in a swirl recovery. At a medium thrust condition the integrated reduction in swirl kinetic energy equaled 50%, with the largest reductions obtained at the inboard radial stations. Analysis of the axial velocity profiles downstream of the vanes and the contraction of the slipstream at all considered operating conditions indicated a potential increase in thrust due to installation of the SRVs. However, because of the asymmetric configuration with SRVs installed it was concluded that the data acquired in the single measurement plane could not be used to quantify the overall gains in system thrust and efficiency.
- The out-of-flow microphone data showed that with the SRVs present the total sound pressure levels were increased by 2 to 6 dB compared to the isolated propeller. Considering the limited upstream effect of the SRVs on the rotor, it is concluded that this noise penalty is mainly the result of the additional noise generating mechanism due to the periodic impingement of the rotor blade wakes. Proper consideration of the acoustics in the design process of the SRVs could reduce the noise penalty resulting from their installation.

The scope of the experimental analysis discussed in this manuscript was limited to the effects of installation of the SRVs at system level, only taking into account the propeller and the vanes. Currently, a more extensive research program is being performed at Delft University of Technology in which the overall performance effects are considered. In this case, the contribution of the SRVs to the overall propulsive efficiency are investigated taking into account the lift and drag loading of the trailing wing for a tractor propeller aircraft lay-out. Also, the design code used to define the vane geometry is undergoing improvements which should further enhance the swirl recovery performance of future designs.

Acknowledgments

The results presented in this paper were obtained by the APIAN-INF research partners in the framework of the transnational access program organized by the ESWIRP consortium, as part of the ESWIRP project (European Strategic Wind tunnels Improved Research Potential). The research leading to these results has received funding from the European Union Seventh Framework Programme (FP7-INFRASTRUCTURE-2008-1) under grant agreement n° 227816.

References

[1]Hager, R. and Vrabel, D., "Advanced Turboprop Project," 1988, NASA-SP-495.

[2]Schnell, R., Yin, J., and Nicke, E., "Assessment and Optimization of the Aerodynamic and Acoustic Characteristics of a Counter Rotating Open Rotor," *Journal of Turbomachinery*, Vol. 134, No. 6, 2012.

[3]Stürmer, A., Márquez Gutierrez, C. O., Roosenboom, E. W. M., Schröder, A., Geisler, R., Pallek, D., Agocs, J., and Neitzke, K., "Experimental and Numerical Investigation of a Contra-Rotating Open Rotor Flowfield," *Journal of Aircraft*, Vol. 49, No. 6, 2014, pp. 1868–1877.

[4]Parry, A. B., Britchford, K. M., Kingan, M. J., and Sureshkumar, P., "Aeroacoustic Tests of Isolated Open Rotors at High Speed," *18th AIAA/CEAS Aeroacoustics Conference*, 2012, Colorado Springs, CO, USA.

[5]Ricouard, J., Julliard, E., Omaïs, M., Regnier, V., Parry, A. B., and Baralon, S., "Installation effects on contra-rotating open rotor noise," *16th AIAA/CEAS Aeroacoustics Conference*, 2010, Stockholm, Sweden.

[6]Stürmer, A. and Yin, J., "Progress in aerodynamic and aeroacoustic integration of CROR propulsion systems," *The Aeronautical Journal*, Vol. 118, No. 1208, 2014, pp. 1137–1158.

[7]Colin, Y., Wlassow, F., Caruelle, B., Nodé-Langlois, T., Omaïs, M., Spiegel, P., and Parry, A. B., "Installation Effects on Contra-Rotating Open Rotor Noise at High-Speed," *20th AIAA/CEAS Aeroacoustics Conference*, 2014, Atlanta, GA, USA.

[8]Paquet, C., Julliard, E., Genoulaz, N., Ricouard, J., and Spiegel, P., "Z08: low-speed aero-acoustic experimental characterization of open rotor installation on aircraft," *20th AIAA/CEAS Aeroacoustics Conference*, 2014, Atlanta, GA, USA.

[9]Czech, M. J. and Thomas, R. H., "Open Rotor Aeroacoustic Installation Effects for Conventional and Unconventional Airframes," *19th AIAA/CEAS Aeroacoustics Conference*, 2013, Berlin, Germany.

[10]Kennedy, J., Eret, P., and Bennett, G. J., "A parametric study of installed counter rotating open rotors," *19th AIAA/CEAS Aeroacoustics Conference*, 2013, Berlin, Germany.

[11]Strack, W. C., Knip, G., Weisbrich, A. L., Godston, J., and Bradley, E., "Technology and Benefits of Aircraft Counter Rotation Propellers," 1982, NASA-TM-82983.

[12]Gazzaniga, J. and Rose, G., "Wind tunnel performance results of swirl recovery vanes as tested with an advanced high speed propeller," *28th Joint Propulsion Conference & Exhibit*, 1992, Nashville, TN, USA.

[13]Miller, C. J., "Euler Analysis of a Swirl Recovery Vane Design for Use With an Advanced Single-Rotation Propfan," *24th Joint Propulsion Conference & Exhibit*, 1988, Boston, MA, USA.

[14]Yamamoto, O., "Numerical Calculation of Propfan/Swirl Recovery Vane Flow Field," *28th Joint Propulsion Conference & Exhibit*, 1992, Nashville, TN, USA.

[15]Dittmar, J. H. and Hall, D. G., "Cruise Noise of an Advanced Propeller with Swirl Recovery Vanes," *Journal of Aircraft*, Vol. 30, No. 2, 1993, pp. 221–226.

[16]Yangang, W., Qingxi, L., Eitelberg, G., Veldhuis, L. L. M., and Kotsonis, M., "Design and numerical investigation of swirl recovery vanes for the Fokker 29 propeller," *Chinese Journal of Aeronautics*, Vol. 27, No. 5, 2014, pp. 1128–1136.

[17]Sinnige, T., Lynch, K. P., Ragni, D., Eitelberg, G., and Veldhuis, L. L. M., "Aerodynamic and Aeroacoustic Effects of Pylon Trailing Edge Blowing on Pusher Propeller Installation," *21st AIAA/CEAS Aeroacoustics Conference*, 2015, Dallas, TX, USA.

[18]Holthusen, H., Bergmann, A., and Sijtsma, P., "Investigations and measures to improve the acoustic characteristics of the German-Dutch Wind Tunnel DNW-LLF," *18th AIAA/CEAS Aeroacoustics Conference*, 2012, Colorado Springs, CO, USA.

[19]Polacsek, C., Spiegel, P., Boyle, F., Eaton, J., Brouwer, H., and Nijboer, R., "Noise Computation of High-Speed Propeller-Driven Aircraft," *6th AIAA/CEAS Aeroacoustics Conference*, 2000, Lahaina, HI, USA.

[20]Bousquet, J.-M. and Gardarein, P., "Recent improvements in Propeller Aerodynamic computations," *18th AIAA Applied Aerodynamics Conference*, 2000, Denver, CO, USA.

[21]Philipsen, I., Hoeijmakers, H., and Hegen, S., "An Overview of Advanced Propeller Simulation Tests in the German Dutch Wind Tunnels (DNW)," *22nd AIAA Aerodynamic Measurement Technology and Ground Testing Conference*, 2002, St. Louis, MO, USA.

[22]Crozier, P., "APIAN Installed Tests in the ONERA S1MA Wind Tunnel," *39th AIAA Aerospace Sciences Meeting & Exhibit*, 2001, Reno, NV, USA.

[23]Drela, M. and Youngren, H., "XROTOR: an interactive program for the design and analysis of ducted and free-tip propellers and windmills," 2011, [Software] Available at: `http://web.mit.edu/drela/Public/web/xrotor`. [Accessed 13 November 2014].

[24]Hanson, D., "Noise of Counter-rotation Propellers," *Journal of Aircraft*, Vol. 22, No. 7, 1985, pp. 609–617.

[25]Groeneweg, J. F., Sofrin, T. G., Rice, E. J., and Gliebe, P. R., "Turbomachinery Noise," *Aeroacoustics of Flight Vehicles: Theory and Practice - Volume 1: Noise Sources*, edited by H. H. Hubbard, National Aeronautics and Space Administration, 1991.

[26]Woodward, R. P., Elliott, D. M., Hughes, C. E., and Berton, J. J., "Benefits of Swept-and-Leaned Stators for Fan Noise Reduction," *Journal of Aircraft*, Vol. 38, No. 6, 2001, pp. 1130–1138.